Rapid Airplane Parametric Input Design (RAPID) *

Robert E. Smith†
Malcolm I. G. Bloor‡
Michael J. Wilson§
Almuttil M. Thomas¶

ABSTRACT

An efficient methodology is presented for defining a class of airplane configurations. Inclusive in this definition are surface grids, volume grids, and grid sensitivity. A small set of design parameters and grid control parameters govern the process. The general airplane configuration has wing, fuselage, vertical tail, horizontal tail, and canard components. The wing, tail, and canard components are manifested by solving a fourth-order partial differential equation subject to Dirichlet and Neumann boundary conditions. The design variables are incorporated into the boundary conditions, and the solution is expressed as a Fourier series. The fuselage has circular cross section, and the radius is an algebraic function of four design parameters and an independent computational variable. Volume grids are obtained through an application of the Control Point Form method. Grid sensitivity is obtained by applying the automatic differentiation precompiler ADIFOR to software for the grid generation. The computed surface grids, volume grids, and sensitivity derivatives are suitable for a wide range of Computational Fluid Dynamics simulation and configuration optimizations.

NOMENCLATURE

$\mathbf{A}$	Vector Fourier coefficients
$\mathbf{B}$	Vector Fourier coefficients
$\mathbf{D}$	Vector Dirichlet boundary conditions
$\mathbf{N}$	Vector Neumann boundary conditions
$\mathbf{X}$	Surface coordinate
$\mathbf{X}_{surf}$	Surface grid
$\mathbf{X}_{vol}$	Volume grid
$\mathbf{a}$	Vector constant for Fourier expression
$\mathbf{b}$	Vector constant for Fourier expression
B_t	Root chord length for tail components
B_w	Root chord length for wing component
B_c	Root chord length for canard component
C	Wing chord length at crank
E	Wingtip chord length
F_1, F_2	Parameters for airfoil definition
H_1	Inboard wing span length
H_2	Outboard wing span length
K_1, K_2	Constants for grid spacing control
K_3, K_4	Constants for grid spacing control
M	Maximum wing camber
P	Location of maximum wing camber
R_F	Fuselage length
R_0, R_1	Parameters for fuselage radius
R_2	Parameter for radius at rearmost point
S_1, S_2	Derivative control design parameters
T	Maximum wing thickness
T_a	Wing taper parameter
X_t, Z_t	Coordinates of trailing tip point
X_w, Z_w	Coordinates of trailing wing point
X_c, Z_c	Coordinates of trailing crank point
a	PDE weighting factor
r	Fuselage radius
$\bar{x}$	Airfoil independent variable
$\bar{y}$	Airfoil dependent variable
$\bar{y}_c$	Wing camber
$\bar{y}_t$	Wing thickness
σ	Coordinate weighting parameter

† Senior Research Engineer , NASA Langley Research Center, Hampton Virginia 23681-0001, Associate Fellow, AIAA.

‡ Professor, Department of Applied Mathematics Studies, University of Leeds, Leeds LS2 9JT, UK.

§ Senior Lecturer, Department of Applied Mathematics Studies, University of Leeds, Leeds LS2 9JT, UK.

¶ Graduate Assistant, Department of Mechanical Engineering, Old Dominion University, Norfolk, Virginia 23529-0247.

ξ, η, ζ	Computational coordinates
$\bar{\xi}, \bar{\eta}, \bar{\zeta}$	Computational coordinates
ν	Grid spacing control coordinate
$\bar{\nu}$	Grid spacing control coordinate
θ	Fuselage definition variable
$\mathcal{P}$	Set of design parameters
$\mathcal{K}$	Set of grid control parameters
Indices	
I	ith point
J	jth point
K	kth point
n	Index for Fourier series

1. INTRODUCTION

Airplane design has historically been divided into three phases: (1) conceptual design; (2) preliminary design; and (3) detailed design[1,2,3]. The conceptual design of an airplane usually begins with specifications for a proposed mission and rough sketches of the configuration. Geometry begins to evolve in the form of sets of connected points. Usually only the minimal amount of information for low-level analyses is created. As a configuration approaches the end of the conceptual design phase, Computer-Aided Design (CAD) models are created. CAD models are most often derived by interpolating and refining the earlier specified sets of connecting points used in low-level analyses.

In the preliminary-design phase, high-level analysis and testing of physical models are performed. Geometry for computational analysis and the construction of test models is extracted from the CAD model. Usually the airplane surface geometry is fixed except for the occasional change that may result from the new analyses, and these changes are implemented in the CAD model. In the detailed-design phase, the CAD model is the central design representation, now containing detailed information for manufacturing the airplane[1].

It can be argued that a CAD model should be implemented at the very earliest stage of conceptual design. However, conventional CAD models and CAD software are very general and very complex. Usually a CAD specialist is required to implement the software. In an environment where the ability to quickly change features of the geometry is nearly as important as the geometry itself, it is desirable: (1) to have the geometry model specified in terms of a small number of design parameters; (2) to visualize the geometry and interact with it to explore the envelope of possibilities; and (3) to quickly extract grids and grid sensitivity for automated analysis (both low-level and high-level) and optimization. As the geometry becomes detailed, it is imperative that a CAD model, with its general characteristics be developed, and any parameter-defined model should be upgraded with a conventional CAD system. Alternately, it would be desirable to incorporate a methodology like the one described here in a conventional CAD system.

Creating an airplane surface or any other object surface with design parameters implies that there is an underlining set of rules or correspondences (model functions) that are driven by the parameters and independent computational variables. Surfaces grids are discrete evaluations of the surface functions, and surface grids can be described as organized sets of points. Different discipline analyses and different techniques within a discipline most often require different grids to be generated from the surface model[4].

High level aerodynamic analysis, such as Euler or Navier-Stokes simulation, require that volume grids be constructed about the configuration surface grid. Information, such as far-field boundary surfaces and grid spacing controls to capture anticipated physics, is required. Surface grids that are generated for low-level analyses usually are not suitable to directly connect to a surrounding volume grid. Interpolation or reevaluation of the surface grid is most often required before proceeding to high-level analysis[5].

The sensitivity of mission dependent variables with respect to design variables is a desired and often used feature in the design process. An intermediate requirement for many techniques is surface-grid and volume-grid sensitivity with respect to the design variables[6].

In this paper, a methodology to define a class of airplane configurations and directly evaluate surface grids, volume grids, and grid sensitivity is presented. The objective of the methodology is to provide surface definition and grid generation for conceptual design that could be used in a wide spectrum of analyses (potential flow to Navier-Stokes). The methodology and associated software is called Rapid Airplane Parametric Input Design (RAPID). The general configuration, at this writing, has wing, fuselage, vertical tail, horizontal tail, and canard components (Fig. 1).

The definition of the lifting surfaces is based on the PDE method as described by Bloor and Wilson[7,8]. Design parameters are incorporated into boundary conditions for the PDE solution. The fuselage has circular cross section and is defined with an algebraic function.

2. THE PDE METHOD

The PDE method generates a Euclidean Space surface $\mathbf{X} = (x(\xi,\eta),\ y(\xi,\eta),\ z(\xi,\eta))$ transformed from $(0 \le \xi \le 1) \times (0 \le \eta \le 1)$ computational space. The transformation is obtained by solving the fourth order partial differential equation

$$\left[a^2 \frac{\partial^2}{\partial \xi^2} + \frac{\partial^2}{\partial \eta^2}\right]^2 \mathbf{X} = 0. \tag{1}$$

By letting $(0 \le \xi \le 1) \rightarrow (0 \le \xi \le 2\pi)$, a general periodic solution to Eq. 1 is:

$$\mathbf{X}(\xi,\eta) = \mathbf{A}_0 + \sum_{n=1}^{\infty} \mathbf{A}_n(\eta) cos(n\xi) + \mathbf{B}_n(\eta) sin(n\xi), \tag{2}$$

where

$$\mathbf{A}_0 = \mathbf{a}_{00} + \mathbf{a}_{01}\eta + \mathbf{a}_{02}\eta^2 + \mathbf{a}_{03}\eta^3,$$

$$\mathbf{A}_n = \mathbf{a}_{n1}e^{an\eta} + \mathbf{a}_{n2}\eta e^{an\eta} + \mathbf{a}_{n3}e^{-an\eta} + \mathbf{a}_{n4}\eta e^{-an\eta},$$

$$\mathbf{B}_n = \mathbf{b}_{n1}e^{an\eta} + \mathbf{b}_{n2}\eta e^{an\eta} + \mathbf{b}_{n3}e^{-an\eta} + \mathbf{b}_{n4}\eta e^{-an\eta}.$$

$\mathbf{a}_{n1}$, $\mathbf{a}_{n2}$, $\mathbf{a}_{n3}$, $\mathbf{a}_{n4}$ and $\mathbf{b}_{n1}$, $\mathbf{b}_{n2}$, $\mathbf{b}_{n3}$, $\mathbf{b}_{n4}$ are vector-valued constants determined by the boundary condition imposed at $\eta = 0$ and $\eta = 1$. The boundary conditions are:

$$\mathbf{X}(\xi,0) = \mathbf{D}_0(\xi), \qquad \mathbf{X}(\xi,1) = \mathbf{D}_1(\xi),$$

$$\mathbf{X}_\eta(\xi,0) = \mathbf{N}_0(\xi), \qquad \mathbf{X}_\eta(\xi,1) = \mathbf{N}_1(\xi).$$

Incorporating a set of design parameters $\mathcal{P}$ in the boundary conditions controls the shape of the surface.

For the family of airplanes described herein, two PDE surfaces define the wing (Fig.2). Boundary conditions are specified at: (1) the wing/fuselage intersection; (2) the crank between the inboard-wing component and outboard-wing component; and (3) the wingtip. The horizontal tail, vertical tail and cannard components are each described with a single PDE surface with boundary condition at the fuselage intersections and at the tips. The PDE boundary conditions are detailed in Section 4.

3. FUSELAGE SURFACE

The fuselage definition in the RAPID methodology is an algebraic function which creates two surfaces - one above the fuselage intersection with the lifting components and one below (Fig. 3). The airplane is considered to be symmetric about the xz plane at $y = 0$, and only one side of the airplane surface is computed. The fuselage cross section is circular, and both the upper and lower surfaces can be represented as $\mathbf{X} = (x(\xi,\zeta), y(\xi,\zeta), z(\xi,\zeta))$ where

$$x = R_F\xi, \quad y = r(\xi)cos(\pi\zeta/2), \quad z = \pm r(\xi)sin(\pi\zeta/2),$$

$$r(\xi) = R_0 sin(\theta) + R_1 sin(3\theta),$$

$$\theta = \pi((1 - R_2)\xi + R_2),$$

$$0 \le \xi \le 1, \qquad 0 \le \zeta \le 1. \tag{3}$$

$\xi = 0$ corresponds to the end point on the fuselage, and $\zeta = 0$ corresponds to a point along the curve separating the upper and lower fuselage surfaces (Fig. 3).

The parameters for the fuselage are: R_F, the fuselage length; R_0 and R_1, control for the fuselage radius; and R_2, a parameter to control a finite radius at the end of the fuselage. The boundary curve separating the upper and lower fuselage surfaces is a combination of the fuselage intersection with the lifting components and cubic curves connecting the intersections. The fuselage center is optionally allowed to translate upward along a quadratic function from the trailing wing/fuselage intersection point to the end of the fuselage. This creates a "duck tail" characteristic in the fuselage (Fig. 4).

A surface grid is created by evaluating the surface functions at discrete $\xi(I)$ and $\zeta(K)$. In order to concentrate the grid in certain regions, such as around the wing/fuselage intersection, it is necessary to create control functions that map $0 \le \bar{\xi}, \bar{\zeta} \le 1$ into $0 \le \xi, \zeta \le 1$. The grid control functions and the grid control parameters used in RAPID for this purpose are discussed in a Section 5.

4. PDE BOUNDARY CONDITIONS

Two PDE surfaces are used in RAPID to create a wing. Each surface is computed in a subroutine. The input is an evaluation of the Dirichlet and Neumann boundary conditions $\mathbf{D}_0(\xi(I))$, $\mathbf{N}_0(\xi(I))$, $\mathbf{D}_1(\xi(I))$, $\mathbf{N}_1(\xi(I))$, and $\eta(J)$ chosen to ensure tangent continuity between adjoining surface. Spacing control in the η direction is achieved by mapping

$0 \le \bar{\eta} \le 1 \rightarrow 0 \le \eta \le 1$ prior to the surface evaluation. Grid spacing is discussed in the Section 5. The PDE output is a surface grid $\mathbf{X}(I,J)$ which can be visualized, used for volume grid computation about the airplane, or used in an analysis of the airplane.

The manipulation of a single airfoil section is currently applied in RAPID for all of the Dirichlet conditions. The section is governed by design parameters and is scaled, rotated and translated into different boundary positions with additional parameters. The airfoil section is defined by the sum of a camber curve and a thickness curve (Fig 6). The airfoil equations are:

$$\bar{x}(\xi) = C sin\pi\xi, \qquad \bar{y}(\xi) = \bar{y}_t(\xi) + \bar{y}_c(\xi),$$

$$\bar{y}_t(\xi) = -\frac{T}{2}(sin2\pi\xi + F_1 sin4\pi\xi + F_2 sin6\pi\xi),$$

$$\bar{y}_c(\xi) = \frac{M}{P^2}(2P sin\pi\xi - (sin\pi\xi)^2), \qquad x \le P,$$

$$\bar{y}_c(\xi) = M\frac{(1-2P+2P sin\pi\xi - (sin\pi\xi)^2)}{(1-P)^2} \quad x \ge P,$$

$$0 \le P \le 1, \qquad 0 \le \xi \le 1. \qquad (4)$$

The design parameters for the section are: C, the section chord length; T, the section manimun thickness; F_1 and F_2, Fourier coefficients; M, maximum camber; P, location of maximum camber. The definition of the section starts at the trailing point, proceeds beneath the camber curve, around the leading point and over the camber curve back to the trailing point. The location of maximum camber is measured from the trailing point.

Given the basic wing section, the Dirichlet boundary condition for the two wing components can be expressed. Boundary $\eta = 0$ for the inboard surface is at the crank, and the $\eta = 1$ boundary is at the wing/fuselage intersection (Fig. 5). For the outboard wing component the $\eta = 0$ boundary is at the wing tip and the $\eta = 1$ boundary is at the crank. The crank Dirichlet boundary condition is:

$$\mathbf{D}_0^{in}(\xi) = \mathbf{D}_1^{out}(\xi) = \begin{bmatrix} x = \bar{x}(\xi) + X_c \\ y = R_0 + H_1 \\ z = \bar{y}(\xi) + Z_c \end{bmatrix}, \qquad (5)$$

where (X_c, Z_c) translates the crank boundary in a xz plane at $y = R_0 + H_1$ and H_1 is the span length of the inboard wing component. The Dirichlet boundary condition for this component at the wing/fuselage intersection is:

$$\mathbf{D}_1^{in}(\xi) = \begin{bmatrix} x = \frac{B_w}{C}\bar{x}(\xi) + X_w \\ y = \sqrt{r(\xi_F)^2 - z^2} \\ z = \bar{y}(\xi)T_a + Z_w \end{bmatrix}. \qquad (6)$$

B_w is the wing-root chord length, X_w and Z_w translate the wing/fuselage intersection, and T_a scales the thickness at the wing/fuselage intersection relative to the thickness at the crank. The ξ-location on the fuselage corresponding to the intersection is:

$$\xi_F = \frac{B_w}{R_F C}\bar{x}(\xi) + \frac{X_w}{R_F}.$$

The Dirichlet boundary condition for the outboard wing surface at the wing tip is:

$$\mathbf{D}_0^{out}(\xi) = \begin{bmatrix} x = \frac{E}{C}\bar{x}(\xi) + X_t \\ y = R_0 + H_1 + H_2 \\ z = \frac{E}{C}\bar{y}(\xi) + Z_t \end{bmatrix}. \qquad (7)$$

E is the chord length at the wing tip; X_t and Z_t translates the wing tip in the xz-plane; and H_2 is the span length of the outboard-wing component.

The Neumann boundary condition for both the inboard- and outboard-wing surface at the crank is:

$$\mathbf{N}_0^{in}(\xi) = \mathbf{N}_1^{out}(\xi) = \begin{bmatrix} \frac{\partial x}{\partial \eta} = \frac{S_1}{2}\bar{x}(\xi) \\ \frac{\partial y}{\partial \eta} = -S_1 \\ \frac{\partial z}{\partial \eta} = 0 \end{bmatrix}. \qquad (8)$$

S_1 is a design parameter which affects the transition between the inboard and outboard wing components.

The Neumann boundary condition applied at the wing/fuselage intersection is:

$$\mathbf{N}_1^{in} = \begin{bmatrix} \frac{\partial x}{\partial \eta} = S_2 sin\pi\xi\frac{\partial \bar{y}}{\partial \xi} \\ \frac{\partial y}{\partial \eta} = \frac{\frac{\partial x}{\partial \xi} r(\xi_F)\frac{\partial r}{\partial x} + z\frac{\partial z}{\partial \eta}}{y} \\ \frac{\partial z}{\partial \eta} = -S_2 sin\pi\xi\frac{\partial \bar{x}}{\partial \xi} \end{bmatrix}. \qquad (9)$$

where S_2 is a design parameter affecting the transition of the wing into the fuselage.

The Neumann boundary condition at the wing tip is zero in current RAPID software.

The tail and cannard components are described in a similar fashion with a single surface, and the details are not presented. There are numerous choices of boundary conditions to achieve a desired effect in the lifting surfaces. Those described here represent only one choice that is incorporated into RAPID software.

5. GRID SPACING CONTROL

The evaluation of the equations presented in the previous two sections results in surface grids. An H-type topology is chosen for the general airplane surface and volume grid definition. The proper spacing of grid points within the topology constraints is very important for achieving acceptable accuracy in the application of a flow analysis about the vehicle surface. A double exponential function[9] which maps the computational variables ξ, η, and ζ onto themselves is used in the RAPID methodology. The grid spacing control function is:

$$\nu = K_1 \frac{e^{\frac{K_2}{K_3}\bar{\nu}} - 1}{e^{K_2} - 1},$$

$$0 \le \bar{\nu} \le K_3, \qquad 0 \le \nu \le K_1,$$

$$\nu = K_1 + (1 - K_1)\frac{e^{K_4 \frac{\bar{\nu} - K_3}{1 - K_3}} - 1}{e^{K_4} - 1},$$

$$K_3 \le \bar{\nu} \le 1, \quad K_1 \le \nu \le 1,$$

$$K_4 \quad chosen \quad \ni \quad \frac{D\nu(K_3)}{D\bar{\nu}} \quad \subset \quad C^1. \qquad (10)$$

Fig. 7 is used to help describe the grid control parameters K_1, K_2, K_3, and K_4. K_1 and K_3 are coordinates of a point in the unit square. $\bar{\nu}$ is the independent computational variable and corresponds to the percentage of grid points in a particular direction. ν is the dependent computational variable and corresponds to the percentage of distance in the physical space along a grid curve. K_2 and K_4 are coefficients in the exponential functions defined for a particular part of the unit square. Where there is low slope in the control functions, there is a concentration in the grid points, and where there is high slope, there is dispersion in the grid points. In the RAPID methodology Eq. 10 is used several times. The approach specifies a desired spacings at the $\bar{\nu} = 0$ and/or at $\bar{\nu} = 1$ and/or K_3. K_1, K_2,and K_4 are determined by a Newton-Raphson process while satisfying a first derivative continuity condition at (K_3, K_1).

The grid control parameters are distinguished from the configuration design parameters. The design parameters are referred to as the set $\mathcal{P}$, and the grid parameters are referred to as the set $\mathcal{K}$. $\mathcal{K}$ includes the grid spacing parameters described above and the volume grid control points discussed in the Section 6.

6. VOLUME GRID GENERATION

A Control Point Form/Transfinite Interpolation technique[10] is used to compute volume grids for the RAPID methodology. A considerable amount of information has been published on this grid generation method and its variations, and only the major steps are presented here.

Having established a grid on the configuration surface, the volume grid generation is accomplished in four major steps.

Step 1 is the determination of a grid in the symmetry plane. The basic functions used in RAPID are those for Bézier curves computed with the de Casteljau scheme[11]. Control points for an intermediate curve and for a far-field curve are computed from the dimensions of the fuselage (Fig. 8). A set of points are distributed in the ξ-direction on the control curves obtained from the control points. Interpolation from the fuselage surface across the control curves is obtained with a de Casteljau application in the η-computational direction (Fig. 9).

Step 2 is the determination of a three-dimensional grid surface containing the lifting components (Fig. 10). Note that in the H-topology, the top and bottom grids are considered separately. A similar process to that used with the symmetry grid for computing control points from the fuselage and lifting surfaces is applied.

Step 3 is the determination of a cap grid. Control points are extracted from the extreme x and y grid coordinates in the lifting surface grid and the extreme z-grid coordinates in the symmetry plane grid (Fig. 11). The de Casteljau scheme is applied with these control points (Fig. 12).

Step 4 is the application of Transfinite Interpolation to compute the interior grid (Fig. 13).

It is necessary to use several grid-spacing control functions and their control parameters in addition to the interpolation control points in order to achieve a good grid for a given set of design parameters. At this writing, this requires some trial and error before acceptable parameters are realized. However, once an acceptable set of grid parameters $\mathcal{K}$ are found for a given set of design parameters $\mathcal{P}$, small changes in $\mathcal{P}$ do not require changes in $\mathcal{K}$. Therefore, repetitive small changes in the design parameters such as during configuration optimization, does not require the constant modification of the grid parameters. Also note that the volume grids obtained with this algorithm are computed only out to the wing tip. An additional far-field grid would be necessary for most high-level fluid analyses.

An option to using the volume grid generation described above is to use the Coordinate and Sensitivity Calculator for Multidisciplinary Design and Optimization (CSCMDO) process described in Reference 12. In CSCMDO, the RAPID surface grid or a surface grid from some other source is INPUT. The GRIDGEN/CSCMDO software is used to establish an initial volume grid. Thereafter, the initial grid is used by CSCMDO to generate a new volume grid for a new INPUT surface grid. Here again, only small changes in the design parameters can be tolerated without reestablishing the initial grid.

7. GRID SENSITIVITY

Gradient based techniques applied to aerodynamic configurations optimization require the determination of grid sensitivity ($\frac{\partial \mathbf{X}_{vol}}{\partial \mathcal{P}} = \frac{\partial \mathbf{X}_{vol}}{\partial \mathbf{X}_{surf}} \frac{\partial \mathbf{X}_{surf}}{\partial \mathcal{P}}$). In the past in order to evaluate such derivatives, each expression would have to be differentiated and chain ruled through out the mathematical system, either by hand or with the aid of a computer-aided algebraic manipulation system. Fortunately, today there are automatic differentiation programs that differentiate code in other programs. The automatic differentiation program used with RAPID in called Automatic Differentiation for FORTRAN (ADIFOR) developed at the Argonne National Laboratory and Rice University[13]. ADIFOR is a preprocessor which differentiates FORTRAN code. The output of ADIFOR is another FORTRAN code containing both the function evaluation and the derivative evaluations of the function with respect to specified input variables. ADIFOR has been applied to batch versions of the RAPID methodology and is described in Reference 14 for linear aerodynamics optimization. There is also a C-programming language version of ADIFOR which has been applied to CSCMDO.

8. RAPID EXAMPLES

Four RAPID examples are presented to demonstrate the range of application. The examples show only the configuration surfaces.

The first example is shown in Fig. 14. The wing is high relative to the fuselage and has high aspect ratio. The fuselage is relatively short compared to the wing span. The wing is relatively thin and cambered at the mid chord.

The second example is shown in Fig. 15. It is a High-Speed Civil Transport (HSCT) like configuration with a double-delta wing. The leading edge of each wing segment is straight as the result of setting the parameters S_1 and S_2 equal to zero.

The third example is shown in Fig. 16 and is similar to the HSCT configuration. The difference is that the wing now has a single delta planform created with two components.

The fourth example shown in Fig. 17 is another HSCT like configuration. It represents the degree of sophistication that can be incorporated into a RAPID model. The fuselage has a "coke bottle" shape. The wing has dihedral, twist, and the planform is not rectangular. A canard is also included.

9. SUMMARY AND CONCLUSIONS

The RAPID methodology has been outlined for creating airplane configurations for conceptual analysis and optimization. By establishing a grid topology, grid spacing control, semiautomatic volume grid generation, and grid sensitivity a more complete analysis and optimization can be carried out in the conceptual design phase without incurring expensive geometric development. The methodology has considerable versatility and is very computationally efficient.

10. ACKNOWLEDGEMENTS

The authors would like to thank Dr. Jamshid Abolhassani and Mr. Bill Jones, members of the Langley Research Center GEOmetry LABoratory (GEOLAB) for many helpful discussions and assistance with the application of CSCMDO. The first author would also like to thank Dr. Gerald Farin of Arizona State Uni-

versity with whom many helpful and interesting discussions on the topic of this paper were held during the author's sabbatical at ASU in 1994.

11. References

[1] Raymer, D. P., *Aircraft Design: A Conceptual Approach*, AIAA Educational Series, AIAA, 1989.

[2] Nicolai, L., *Fundamentals of Airplane Design*, Distributed by the University of Dayton, Dayton, OH, 1975.

[3] Roskam, J., *Airplane Design*, Rowskam Aviation and Engineering Co., Ottawa, KA, 1989.

[4] Smith, R. E., and Kerr, P. A.,"Geometric Requirements for Multidisciplinary Analysis of Aerospace-Vehicle Design," AIAA Paper 92-4773-CP, Sept. 1992.

[5] Thompson, J., Warsi, Z., and Mastin, C., *Numerical Grid Generation Foundations and Applications*, North-Holland, 1985.

[6] Sobieszczanski-Sobieski, J. "The Case for Aerodynamic Sensitivity Analysis," Paper presented to NASA/VPI SSY Symposium on Sensitivity Analysis in Engineering, September 25-26, 1986.

[7] Bloor, M. and Wilson, M., "Generating Blend Surfaces Using Partial Differential Equations," CAD, 21, No. 3 pp 165-171, 1989.

[8] Bloor, M., and Wilson, M., "Using Partial Differential Equations to Generate Free-Form Surfaces," Computer-Aided Design, 22, pp 202-212, 1990.

[9] Smith, R. and Everton, E., "Interactive Grid Generation for Fighter Aircraft Geometries," *Numerical Grid Generation in Computational Fluid Mechanics '88*, pp. 805-814, Pine Ridge Press Ltd., 1988.

[10] Eiseman, P. R., and Smith, R. E., "Applications of Algebraic Grid Generation , Applications of Mesh Generation to Complex 3-D Configurations," AGARD-CP-464, pp. 4-1-12, 1989.

[11] Farin, G., *Curves and Surfaces for Computer-Aided Geometric Design A Practical Guide*, Academic Press, 1993.

[12] Jones, W., and Samareh-Abolhassani, J., "A Grid Generation System for Multi-disciplinary Design," AIAA Paper 95-1689, June, 1995.

[13] Bischof, C., et. al., "Automatic Differentiation of Advanced CFD Codes for Multidisciplinary Design," *Computer Systems in Engineering* No. 3, pp 625-637, 1993.

[14] Thomas, A., Smith, R., and Tiwari, S., "Aerodynamic Shape Optimization of Blend Surfaces Representing HSCT Type Configurations," AIAA Paper 95-1826, June, 1995.

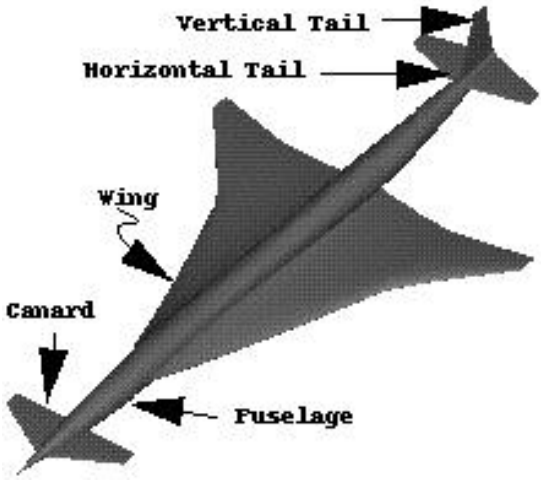

Fig. 1 General airplane configuration

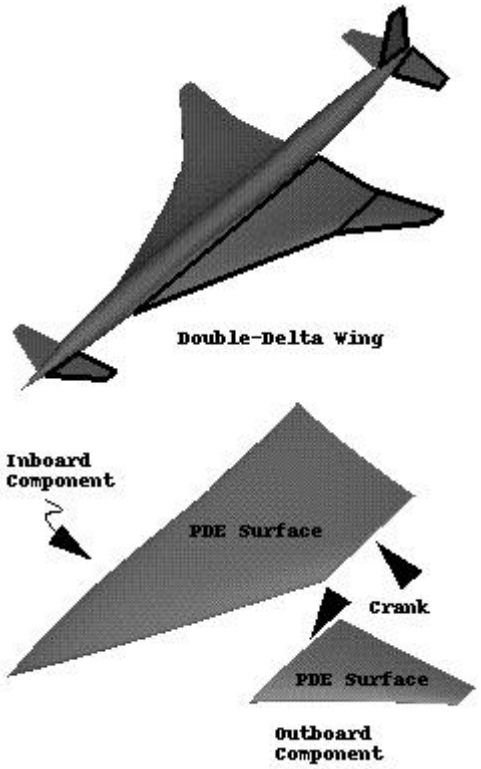

Fig. 2 Configuration surface topology

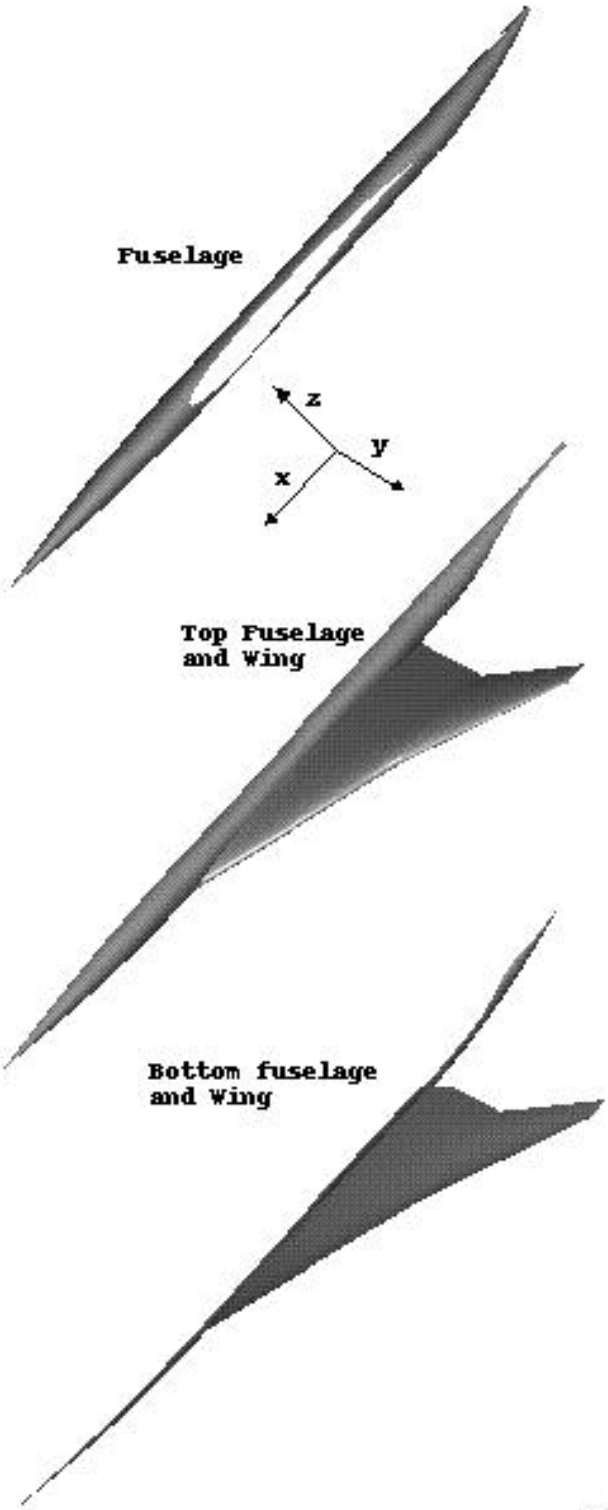

Fig. 3 Fuselage surface and topology

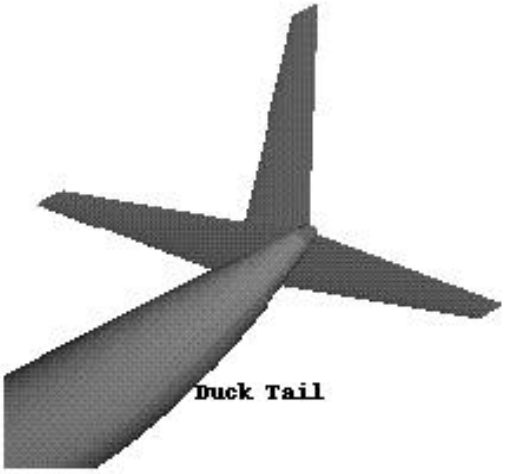

Fig. 4 Duck tail fuselage characteristic

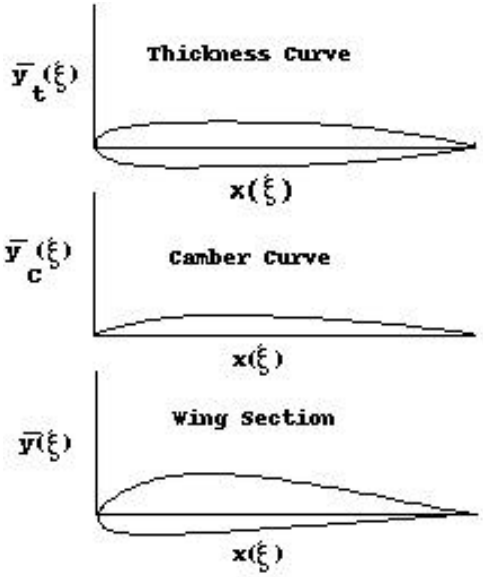

Fig. 5 Wing section definition

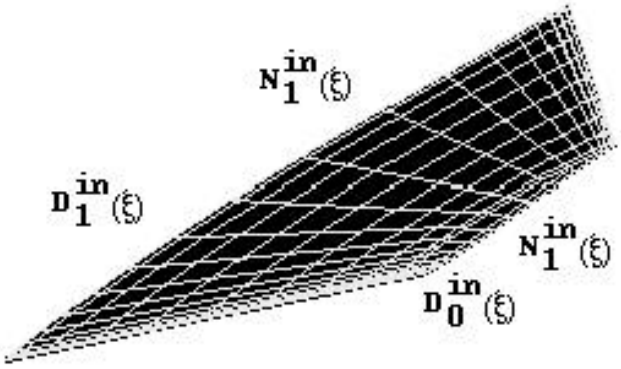

Fig. 6 Wing component boundary conditions

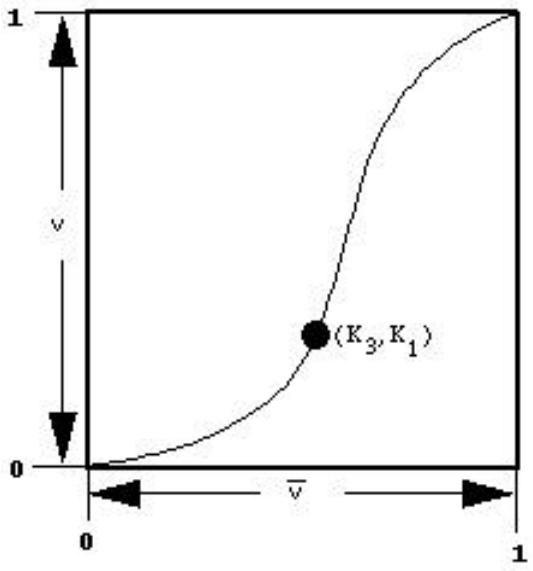

Fig. 7 Grid spacing control function

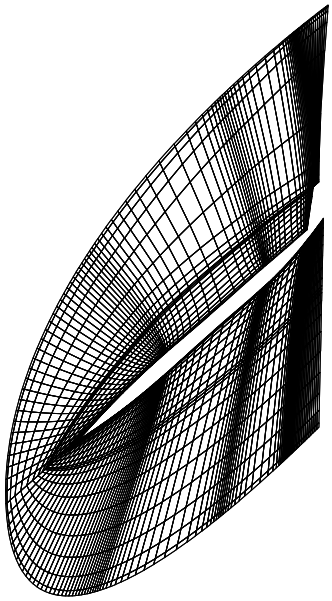

Fig. 9 Symmetry grid

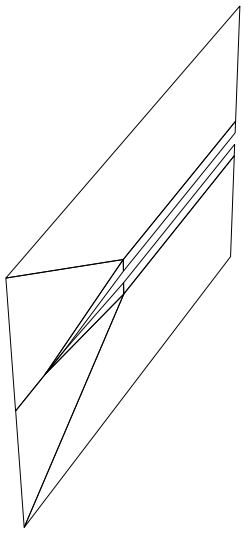

Fig. 8 Symmetry plane control net

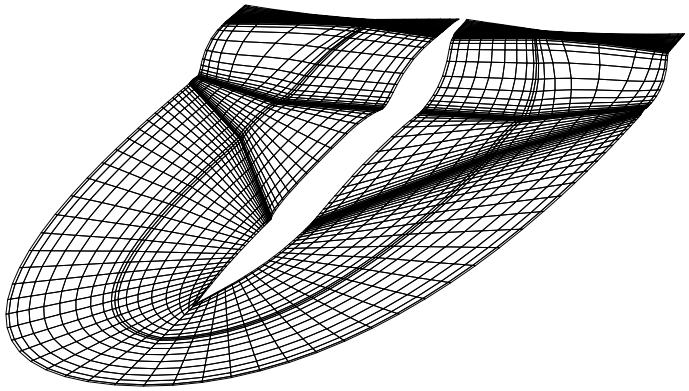

Fig. 10 Surface grid containing lifting components

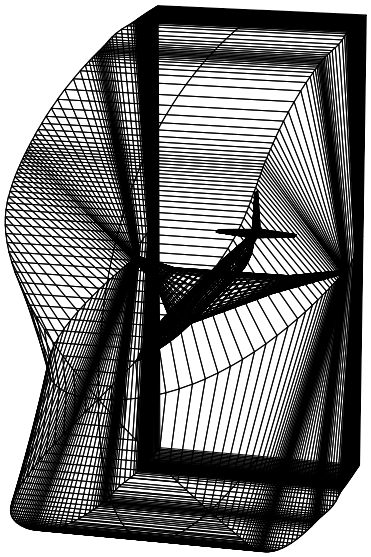

Fig. 11 Control point for outer grid surface

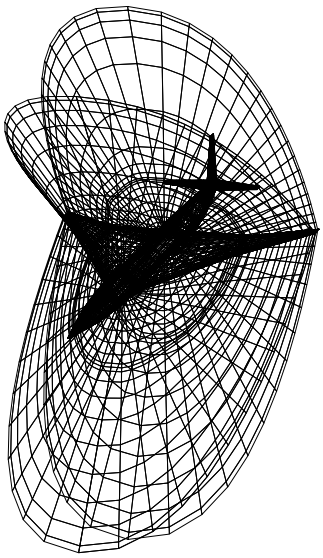

Fig. 13 Sample grid surfaces

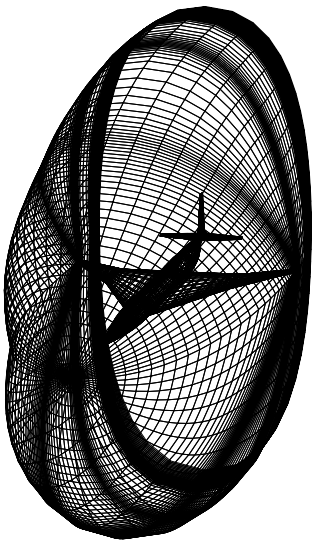

Fig. 12 Outer grid surface

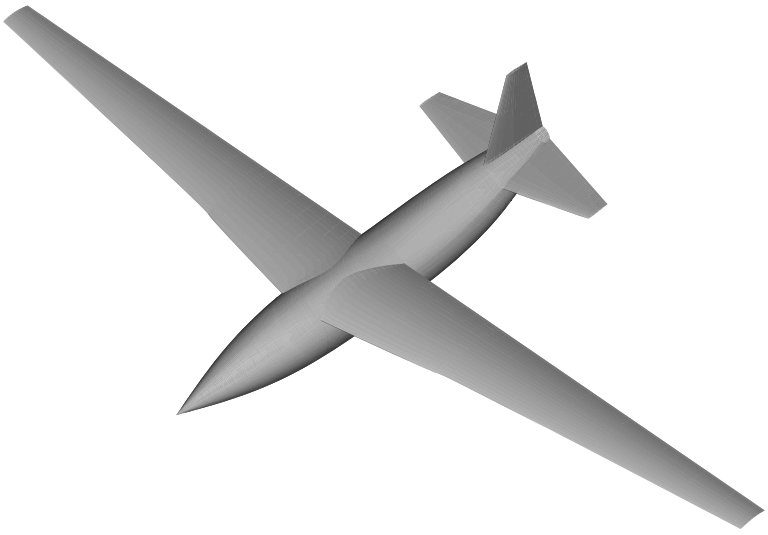

Fig. 14 High wing configuration

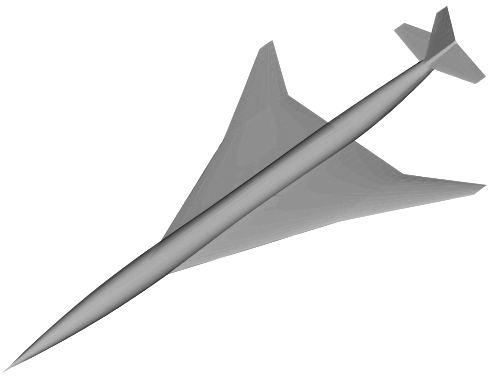

Fig. 15 HSCT configuration

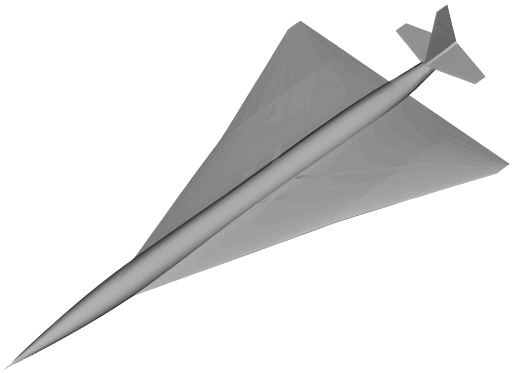

Fig. 16 Delta wing configuration

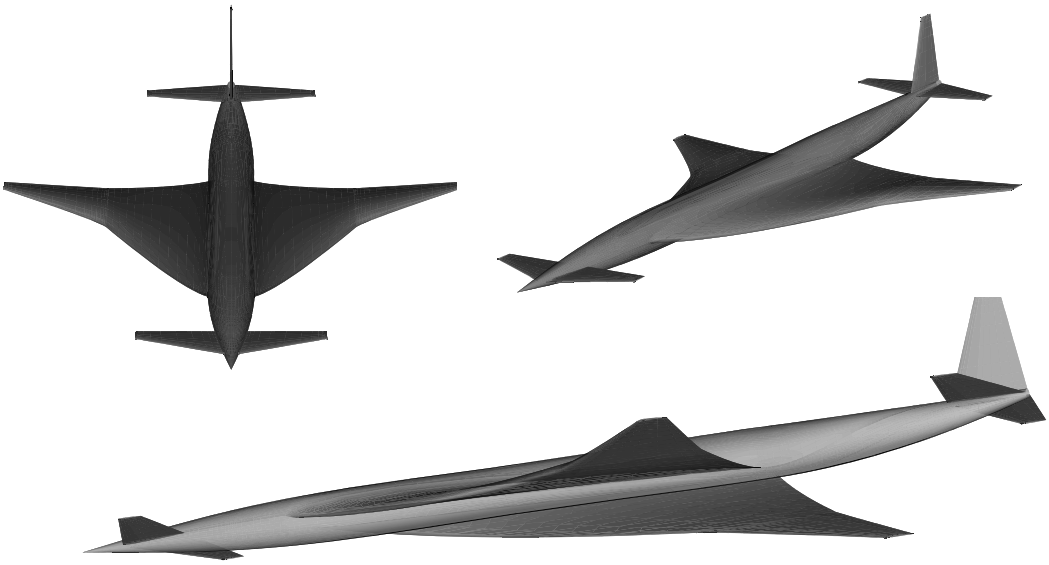

Fig. 17 Canard twisted-wing configuration